View Article Online / Journal Homepage / Table of Contents for this issue
Dynamic Article Links

ChemComm

Cite this: *Chem. Commun.*, 2012, **48**, 1565–1567

www.rsc.org/chemcomm

COMMUNICATION

Atom arrangement strategy for designing a turn-on ^{1}H magnetic resonance probe: a dual activatable probe for multimodal detection of hypochlorite†‡

Tomohiro Doura,[a] Hiroshi Nonaka[a] and Shinsuke Sando*[ab]

Received 11th April 2011, Accepted 27th April 2011
DOI: 10.1039/c1cc12044a

Published on 17 May 2011. Downloaded by Michigan State University on 25/01/2016 15:28:51.

The first dual activatable hypochlorite ($^{-}$OCl)-sensing probe was developed, based on a new proof-of-concept design involving signal-activatable ^{1}H chemical probes using the triple-resonance NMR technique. The probe enabled fluorescence–^{1}H MR dual turn-on detection of $^{-}$OCl in solution and in crude tissue extracts.

Reactive oxygen species (ROS) play important roles in physiological and pathological events in the cell. Consequently, the demand for ROS-sensing and -imaging probes has increased.[1] These probes are powerful tools for elucidating the precise roles of ROS and may also be useful for medical diagnosis.

Most ROS bioimaging tools involve fluorescent probes because they can be used in conjunction with fluorescence microscopy. Activatable fluorescent probes,[2] which are otherwise nonfluorescent but fluoresce upon reaction with the target species, have been developed for direct monitoring of ROS in live cells.[1] Although fluorescent probes have superior sensitivity and spatiotemporal resolution, their use for *ex vivo* and *in vivo* applications is limited by low penetration of excitation or emission light, with the exception of potent near-infrared fluorescence[3] and bioluminescence probes.[4] A magnetic resonance (MR)-based technique such as MR spectroscopy (MRS) or MR imaging (MRI) is appropriate for this purpose because a MR probe could be detected even if it were situated deep within the body.[5] However, the disadvantages of MR are that it has low spatiotemporal resolution compared with the fluorescence-based approach. In this context, ideal chemical probes are those that can be detected in a fluorescence–MR dual-modal fashion so that an appropriate detection mode can be selected depending on the situation, *e.g.*, MR could be used to obtain anatomic information and fluorescence could be used when high spatiotemporal resolution is required on the targeted region.[6,7] Herein, we present the first description of a ROS-sensing probe for fluorescence–^{1}H-MR dual-modal detection. The probe achieved dual turn-on sensing of hypochlorite ($^{-}$OCl) with high specificity.

The first challenge in developing a dual-modal probe for turn-on sensing of ROS is to design a signal-activatable MR probe. Particularly, an activatable ^{1}H-MR probe is attractive for MRS or MRI because ^{1}H has the highest sensitivity of available nuclei. However, ^{1}H detection typically suffers from nonnegligible interference from the high background emanating from a variety of endogenous ^{1}H-containing biological compounds.

To overcome these problems, we focused on a one-dimensional triple-resonance ^{1}H NMR technique. Triple resonance is used to correlate three NMR-active nuclei with different Larmor frequencies[8] and has been applied mostly to structural analysis of biopolymers, except for precedents,[9,10] including studies from our laboratory.[10] For example, when the pulse scheme allows the magnetic coherence of ^{1}H to transfer to two successive ^{13}C nuclei with different Larmor frequencies (^{13}C and ^{13}C′) through scalar couplings, only the ^{1}H in the specific sequence ^{1}H–^{13}C–^{13}C′ is detectable. Therefore, we hypothesized that if we could design a ^{13}C-labelled chemical probe, which initially has no detectable ^{1}H–^{13}C–^{13}C′ atom sequence but develops an active ^{1}H–^{13}C–^{13}C′ sequence upon reaction with ROS, it should function as an *off*-to-*on*-type ^{1}H probe under triple resonance conditions (Fig. 1). This is a completely new mode for designing signal-activatable ^{1}H MR probes.

In addition to signal activation, the triple resonance technique affords selectivity. Because of the low natural abundance of ^{13}C (1.1%), the probability of a naturally occurring ^{1}H–^{13}C–^{13}C′ sequence is $<0.01\%$. Therefore, this technique could markedly improve the selectivity of the target ^{1}H connecting with ^{13}C–^{13}C′ because of low background ^{1}H signals.

Along this concept, we designed ^{13}C-labelled 4-methyl-3,4-dihydrocoumarin (**HCm** in Fig. 2a) as a probe scaffold. Under the NMR pulse sequence of ^{1}H–{^{13}C–^{13}C′$^{(sp2)}$} for detection of an ^{1}H bound to an aliphatic ^{13}C, which in turn is bound to sp2 ^{13}C′$^{(sp2)}$ on a conjugated double bond, **HCm** has no detectable ^{1}H because of the lack of a ^{1}H–^{13}C–^{13}C′$^{(sp2)}$ sequence. On the other hand, if the **HCm** structure is oxidized

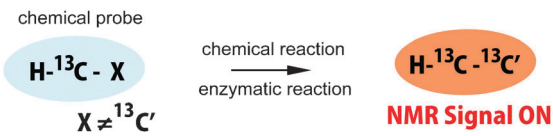

Fig. 1 A strategy for designing a signal activatable ^{1}H MR probe.

[a] *INAMORI Frontier Research Center, Kyushu University, 744 Motooka, Nishi-ku, Fukuoka 819-0395, Japan. E-mail: ssando@ifrc.kyushu-u.ac.jp*
[b] *PRESTO, Japan Science and Technology Agency, 4-1-8 Honcho, Kawaguchi, Saitama 332-0012, Japan*

† This article is part of the 'Emerging Investigators' themed issue for ChemComm.

‡ Electronic supplementary information (ESI) available: Fig. S1–S5 and methods. See DOI: 10.1039/c1cc12044a

View Article Online

Published on 17 May 2011. Downloaded by Michigan State University on 25/01/2016 15:28:51.

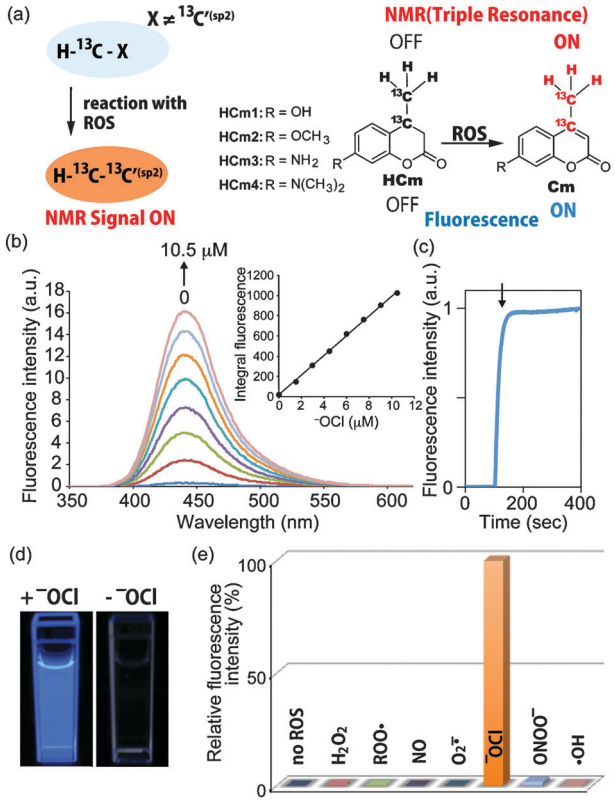

Fig. 2 (a) Chemical structures of 4-methyl-3,4-dihydrocoumarin derivatives (**HCm1–4**) and a hypothesized reaction scheme showing how the dihydrocoumarin probe functions as a dual turn-on probe against ROS. (b) Fluorescence spectra (excitation at 342 nm) of **HCm3** (10 μM) after incubation with $^{-}$OCl (0, 1.5, 3, 4.5, 6, 7.5, 9, 10.5 μM from bottom to top) in phosphate buffer (pH 7.4, 100 mM) containing 150 mM NaCl and 0.1% DMF at 37 °C. Inset: $^{-}$OCl-dependent linear increase of integral fluorescence. (c) Time course of fluorescence intensity of **HCm3** (10 μM, excitation at 342 nm and emission at 442 nm) upon addition of one equivalent of $^{-}$OCl. The arrow indicates the addition of $^{-}$OCl. (d) Fluorescent images of **HCm3** (10 μM) in the absence or presence of three equivalents of $^{-}$OCl. (e) Relative fluorescence intensity (%) of **HCm3** (10 μM) (excitation at 342 nm and emission at 442 nm) incubated with various ROS (3 equivalents) and reactive nitrogen species (RNS, 3 equivalents); fluorescence intensity in the presence of $^{-}$OCl was set at 100%. Typical fluorescence spectra of **HCm3** with various ROS and RNS are shown in Fig. S3 (ESI‡).

by ROS to produce an aromatized coumarin structure (**Cm** in Fig. 2a), the detectable ^{1}H–^{13}C–^{13}C$'^{(sp2)}$ sequence is formed (red atoms in Fig. 2a). Because the coumarin scaffold is a fluorescent chromophore, this compound functions as a dual activatable fluorescence–^{1}H-MR probe against ROS.

First, we investigated whether **HCm** would react with ROS to produce aromatized **Cm** as proposed in Fig. 2a. **HCm** derivatives, where R is OH, OCH_3, NH_2, or $N(CH_3)_2$, were synthesized by hydrogenation of **Cm** derivatives, which were prepared by simple condensation of the corresponding phenols with ethyl acetoacetate. Fluorescence spectra for the otherwise very weakly fluorescent **HCm1–4** were measured after incubation with one equivalent of hypochlorite ($^{-}$OCl) (Fig. S1, ESI‡). **HCm3** afforded the highest fluorescence enhancement (I_{on}/I_{off} (**HCm3**) at 442 nm = 45) among **HCm1–4** (I_{on}/I_{off} (**HCm1**) at 449 nm = 5.5, I_{on}/I_{off} (**HCm2**) at 383 nm = 1.2, and I_{on}/I_{off} (**HCm4**) at 473 nm = 19).[11] The reaction of **HCm3** with $^{-}$OCl was clearly dose-dependent (Fig. 2b) and fast (Fig. 2c). Judging from a comparison with the fluorescence intensity of authentic **Cm3**, it was revealed that approximately 6.1% of **HCm3** (10 μM) was converted to a fluorescent coumarin scaffold by reaction with 3 equivalents of $^{-}$OCl. In addition, a detailed product analysis of the reaction solution (**HCm3** 10 μM,$^{-}$OCl 30 μM) using HPLC-fluorescence suggested that the reacted solution contained several fluorescent products; one was **Cm3** and others were coumarin derivatives produced probably by further reaction of the **Cm3** with excess $^{-}$OCl (Fig. S2a, ESI‡). Although the conversion yield was not so high, the probe allowed a practical $^{-}$OCl detection because of high sensitivity of produced fluorescent coumarins. In fact, the **HCm3** enabled clear off-to-on type visualization of $^{-}$OCl under UV light (Fig. 2d) and reached the detection limit of 0.2 μM under our experimental conditions. In addition, the **HCm3** showed fluorescence enhancement specifically to $^{-}$OCl compared with other biologically important ROS (H_2O_2, ROO$^{\bullet}$, $O_2^{\bullet -}$, and $^{\bullet}$OH) and reactive nitrogen species (RNS; NO and $ONOO^{-}$) (Fig. 2e). When the fluorescence intensity of **HCm3** in the presence of $^{-}$OCl was expressed as 100%, the fluorescence of **HCm3** in the presence of all other species was less than 2% (reaction of 10 μM of **HCm3** with 30 μM of ROS or RNS). Product analyses by HPLC-UV revealed that **HCm3** reacted with most of the ROS tested and produced a variety of products (Fig. S2b, ESI‡). In addition, it was found that the **HCm3** probe was not stable under physiological conditions to give a hydrolysed product (Fig. S2b, ESI‡). However, such products were non-fluorescent except for that produced by reaction with $^{-}$OCl, thus resulting in high specificity in fluorescence analysis (Fig. 2e and Fig. S3, ESI‡).

Having developed an $^{-}$OCl-specific fluorescent **HCm3** probe, we tried to add an ^{1}H-activatable moiety to the probe. As 3,4-$^{13}C_2$-labelled ethyl acetoacetate is commercially available, ^{13}C-labelled **HCm3** (**HCm3-$^{13}C_2$**) and **Cm3** (**Cm3-$^{13}C_2$**) can be synthesized according to the procedure in Scheme 1.

First, we measured the NMR spectra of **Cm3-$^{13}C_2$**. The conventional ^{1}H NMR spectrum of **Cm3-$^{13}C_2$** showed aromatic, amino, and aryl ^{1}H (left in Fig. 3a, $CDCl_3$). In contrast, only aryl ^{1}H was detected in the ^{1}H–{^{13}C–^{13}C$'^{(sp2)}$} triple resonance experiment (right in Fig. 3a, $CDCl_3$); the detection limit was 1 μM in D_2O under our experimental conditions. We then examined $^{-}$OCl detection using **HCm3-$^{13}C_2$** as a probe. Again, our purpose was to develop an *off*-to-*on*-type fluorescence–^{1}H MR dual-modal probe that would ideally be undetected until reaction with the target ROS. The **HCm3-$^{13}C_2$** construct is ideal in this respect. **HCm3-$^{13}C_2$** was silent under the triple resonance ^{1}H conditions (upper spectrum in Fig. 3b). In contrast, a single signal was produced after incubation with $^{-}$OCl (lower spectrum in Fig. 3b) with concomitant fluorescence enhancement (Fig. S4, ESI‡).

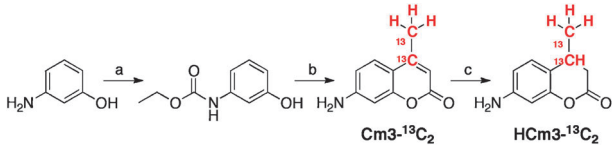

Scheme 1 Synthesis of **HCm3-$^{13}C_2$**. (a) Ethyl chloroformate, Et_2O, rt (48%); (b) (i) ethyl acetoacetate-3,4-$^{13}C_2$, H_2SO_4, rt, (ii) glacial acetic acid, 100 °C (25% in two steps); (c) H_2, Pd–C, EtOH, rt (50%).

 This journal is © The Royal Society of Chemistry 2012

View Article Online

Published on 17 May 2011. Downloaded by Michigan State University on 25/01/2016 15:28:51.

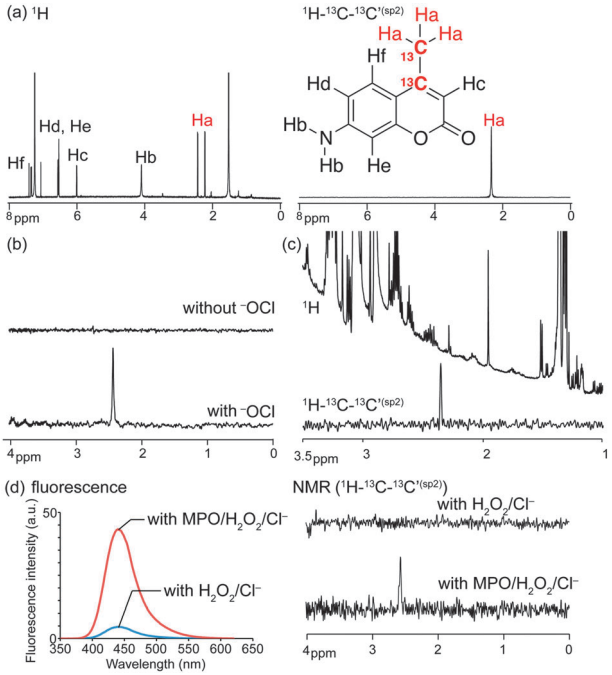

Fig. 3 (a) ^{1}H (left) and ^{1}H–{^{13}C–^{13}C′$^{(sp2)}$} (right) spectra of **Cm3-^{13}C$_2$** (1 mM) in $CDCl_3$. (b) Triple resonance ^{1}H NMR spectra of **HCm3-^{13}C$_2$** (100 μM) incubated with (lower) or without (upper) $^-$OCl (180 μM) in phosphate buffer (pH 7.4, 1 mM) containing 0.1% DMF. (c) Single (^{1}H, upper) and triple resonance (lower) ^{1}H NMR spectra of **HCm3-^{13}C$_2$** (100 μM) incubated with $^-$OCl (800 μM) in the presence of pork muscle extract. (d) Fluorescence (left, excitation at 342 nm) and triple resonance ^{1}H NMR (right) spectra of **HCm3-^{13}C$_2$** (100 μM) after incubation with MPO/H_2O_2/Cl$^-$ or H_2O_2/Cl$^-$.

The signal was confirmed as aryl ^{1}H of the **Cm3-^{13}C$_2$** scaffold by 2D ^{1}H–^{13}C HSQC analysis (Fig. S5, ESI‡), indicating actual production of **Cm3-^{13}C$_2$** or derivatives from **HCm3-^{13}C$_2$** as initially designed. Since the triple resonance technique greatly improves selectivity, $^-$OCl is sensed by **HCm3-^{13}C$_2$** even in crude tissue extracts (lower spectrum in Fig. 3c). On the other hand, detection of generated **Cm3-^{13}C$_2$** or derivatives by conventional ^{1}H NMR was unsuccessful because of spectral overlaps with a variety of ^{1}H signals derived from coexisting molecules (upper spectrum in Fig. 3c). These results clearly indicate that **HCm3-^{13}C$_2$** functions as an *off*-to-*on*-switching ^{1}H MR probe for specific detection of $^-$OCl.

Finally, we applied the **HCm3-^{13}C$_2$** probe to dual-mode detection of myeloperoxidase (MPO) activity. MPO is a heme-containing enzyme present mainly in neutrophils and mediates the production of $^-$OCl from Cl$^-$ and H_2O_2 in the killing of bacteria. As shown in Fig. 3d, **HCm3-^{13}C$_2$** turns on its fluorescence and ^{1}H signal upon incubation with MPO/H_2O_2/Cl$^-$ in an *off*-to-*on* manner. Although the possibility that a fluorescent **Cm3** scaffold was produced by direct oxidation with MPO or reaction with $^1O_2$ generated from MPO cannot be excluded at this stage, this result clearly indicated that our dual turn-on probe is also applicable to sensing of the enzymatic MPO system.

In conclusion, our probe is the first dual activatable fluorescence–^{1}H MR probe for sensing of $^-$OCl. Especially, it should be noted that the ^{1}H MR-based turn-on sensing was achieved using a new proof-of-concept with the triple resonance NMR technique. There are at least three advantages to our method. The first is its selectivity. Because of the low natural abundance of ^{13}C, the ^{1}H–^{13}C–^{13}C′ moiety renders the probe extremely selective. The second advantage is that our probe is signal activatable. Thus, our "switch-on" ^{1}H MR probe is otherwise silent and is rendered active only when a detectable ^{1}H–^{13}C–^{13}C′ sequence is produced upon reacting with the target. The third is versatility. The technique is not limited to H–C–C′$^{(sp2)}$ but can be applied to a variety of atom sequences such as H–C–N. This strategy of "atom arrangement" can be used by chemists who can design and synthesize chemical probes with a variety of atom sequences with different targets.

We demonstrated a new proof-of-concept for designing activatable NMR probes. However, the present probe has room to be improved further, especially in terms of reactivity, conversion yield, and stability under physiological conditions. Further challenge is now in progress in our laboratory.

This work was supported by NEXT program and Grant-in-Aid Number 22685018 from JSPS and performed under the Cooperative Research Program (IMCE, Kyushu University).

Notes and references

1 For a recent review on ROS/RNS imaging probes, see: T. Nagano, *J. Clin. Biochem. Nutr.*, 2009, **45**, 111–124 and references therein.
2 For a recent review on activatable probes, see: H. Kobayashi, M. Ogawa, R. Alford, P. L. Choyke and Y. Urano, *Chem. Rev.*, 2010, **110**, 2620–2640.
3 (*a*) K. Kundu, S. F. Knight, N. Willett, S. Lee, W. R. Taylor and N. Murthy, *Angew. Chem., Int. Ed.*, 2009, **48**, 299–303; (*b*) P. Panizzi, M. Nahrendorf, M. Wildgruber, P. Waterman, J.-L. Figueiredo, E. Aikawa, J. McCarthy, R. Weissleder and S. A. Hilderbrand, *J. Am. Chem. Soc.*, 2009, **131**, 15739–15744; (*c*) D. Oushiki, H. Kojima, T. Terai, M. Arita, K. Hanaoka, Y. Urano and T. Nagano, *J. Am. Chem. Soc.*, 2010, **132**, 2795–2801.
4 S. Gross, S. T. Gammon, B. L. Moss, D. Rauch, J. Harding, J. W. Heinecke, L. Ratner and D. Piwnica-Worms, *Nat. Med. (N. Y.)*, 2009, **15**, 455–461.
5 For ROS-sensitive MR probes, see: (*a*) J. W. Chen, W. Pham, R. Weissleder and A. Bogdanov, *Magn. Reson. Med.*, 2004, **52**, 1021–1028; (*b*) H. Utsumi, K. Yamada, K. Ichikawa, K. Sakai, Y. Kinoshita, S. Matsumoto and M. Nagai, *Proc. Natl. Acad. Sci. U. S. A.*, 2006, **103**, 1463–1468; (*c*) E. Rodríguez, M. Nilges, R. Weissleder and J. W. Chen, *J. Am. Chem. Soc.*, 2010, **132**, 168–177.
6 For a recent review on dual-modal probes, see: L. E. Jennings and N. Long, *Chem. Commun.*, 2009, 3511–3524 and references therein.
7 Recent examples on fluorescence-MR dual-modal probes, see: (*a*) S. Mizukami, R. Takikawa, F. Sugihara, M. Shirakawa and K. Kikuchi, *Angew. Chem., Int. Ed.*, 2009, **48**, 3641–3643; (*b*) Y. You, E. Tomat, K. Hwang, T. Atanasijevic, W. Nam, A. P. Jasanoff and S. J. Lippard, *Chem. Commun.*, 2010, **46**, 4139–4141.
8 L. E. Kay, M. Ikura, R. Tschudin and A. Bax, *J. Magn. Reson.*, 1990, **89**, 496–514.
9 (*a*) J. K. Gard, P. C. C. Feng and W. C. Hutton, *Xenobiotica*, 1997, **27**, 633–644; (*b*) W. C. Hutton, J. J. Likos, J. K. Gard and J. R. Garbow, *J. Labelled Compd. Radiopharm.*, 1998, **41**, 87–95; (*c*) J. K. Gard, W. C. Hutton, J. A. Baker, R. K. Singh and P. C. C. Feng, *Pestic. Sci.*, 1999, **55**, 215–218.
10 K. Mizusawa, R. Igarashi, K. Uehira, Y. Takafuji, Y. Tabata, H. Tochio, M. Shirakawa, S. Sando and Y. Aoyama, *Chem. Lett.*, 2010, **39**, 926–928.
11 For $^-$OCl-selective fluorescence probes, see for example: (*a*) K.-I. Setsukinai, Y. Urano, K. Kakinuma, H. J. Majima and T. Nagano, *J. Biol. Chem.*, 2003, **278**, 3170–3175; (*b*) J. Shepherd, S. A. Hilderbrand, P. Waterman, J. W. Heinecke, R. Weissleder and P. Libby, *Chem. Biol.*, 2007, **14**, 1221–1231; (*c*) S. Kenmoku, Y. Urano, H. Kojima and T. Nagano, *J. Am. Chem. Soc.*, 2007, **129**, 7313–7318; (*d*) ref. 3*b*.